BNL--31957
BNL 31957
DE83 001307
OG651
CONF-820675--4

Measurement of the ν_μ Charged-Current Cross Section

N.J. Baker, P.L. Connolly, S.A. Kahn, M.J. Murtagh, M. Tanaka
Brookhaven National Laboratory, Upton, NY 11973

C. Baltay, M. Bregman, D. Caroumbalis, L.D. Chen, H. French,
M. Hibbs, R. Hylton, P. Igo-Kemenes*, J.T. Liu, J. Okamitsu,
G. Ormazabal, A.C. Schaffer, K. Shastri, J. Spitzer
Columbia University, New York, NY 10027

E.B. Brucker, P.F. Jacques, M. Kalelkar, E.L. Koller,
R.J. Plano, P.E. Stamer, A. Vogel
Rutgers University, New Brunswick, NJ 08903

*on leave from Heidelberg University, Heidelberg, F.R. Germany.

MEASUREMENT OF THE ν_μ CHARGED-CURRENT CROSS SECTION *

N.J. Baker, P.O. Connolly, S.A. Kahn,
M.J. Murtagh, M. Tanaka
Brookhaven National Laboratory, Upton, NY 11973

C. Baltay, M. Bregman, D. Caroumbalis,
L.D. Chen, H. French, M. Hibbs, R. Hylton,
P. Igo-Kemenes, J.T. Liu, J. Okamitsu, G. Ormazabal,
A.C. Schaffer, K. Shastri, J. Spitzer
Columbia University, New York, NY 10027

E.B. Brucker, P.F. Jacques, M. Kalelkar,
E.L. Koller, R.J. Plano, P.E. Stamer, A. Vogel
Rutgers University, New Brunswick, NJ 08903

This paper was presented by P. Igo-Kemenes **

Abstract

The Fermilab 15-ft bubble chamber, filled with a heavy neon-hydrogen mix, was exposed to a narrow band ν_μ beam. Based on the observation of 830 charged current ν_μ interactions, the cross section was found to rise linearly with the neutrino energy in the interval, 10 GeV $\leq E_\nu \leq$ 240 GeV, with a constant slope of:

$$\sigma_\nu/E_\nu = (0.64 \pm 0.05)\ 10^{-38} \text{cm}^2\text{GeV}^{-1} \quad .$$

This result is discussed in relation to other experiments.

1. INTRODUCTION

The cross section of the charged current processes,

$$\nu_\mu + N \rightarrow \mu^- + X$$
$$\tilde{\nu}_\mu + N \rightarrow \mu^+ + X \quad ,$$

for neutrino energies above 10 GeV, was previously determined in several narrow band experiments.[1] With the exception of the Caltech-Columbia-Fermilab-Rochester-Rockefeller (CCFRR) measurement,[2] all experiments gave consistent results on the cross section slopes, σ_ν/E_ν and $\sigma_{\tilde{\nu}}/E_{\tilde{\nu}}$. The comparatively high results obtained by the CCFRR collaboration at the Fermilab narrow band beam increased the interest of the bubble chamber experiments which were taking data concurrently in the same neutrino beam and were using the same neutrino flux monitoring.

* Research supported in part by the Department of Energy and the National Science Foundation.
** On leave from Heidelberg University, Heidelberg, F.R. Germany.

The neutrino data were obtained and analyzed by the BNL-Columbia-Rutgers collaboration and the result on σ_ν/E_ν is the subject of this contribution. The anti-neutrino data were analyzed by the Berkeley-Fermilab-Hawaii collaboration and the result on $\sigma_{\tilde{\nu}}/E_{\tilde{\nu}}$ was also submitted to this conference.[3]

2. THE EXPERIMENT

The layout of the Fermilab narrow band neutrino beam is shown in Fig. 1. The 400 GeV protons hit a beryllium target and produce secondary particles which are momentum and sign selected by the N-30 magnetic train. The source of neutrinos is the decay of secondary pions and kaons along the 340 meter decay pipe. All particles except neutrinos are absorbed in the beam dump and the 910 meter earth shielding which precedes the neutrino detectors. In the figure, the positions of the CCFRR counter experiment and of the 15-ft bubble chamber are indicated.

2.1 Magnetic Train and Neutrino Flux Monitoring

Data were taken with the momentum of the secondary particle beam selected at five different values: 120, 140, 165, 200, and 250 GeV/c. Neutrinos from pion decays covered the energy range $0 \leq E_\nu \leq 80$ GeV and those from kaon decays extended the energy range to 240 GeV.

The neutrino flux at the bubble chamber was obtained from counting the charged secondary particles in ionization chambers situated at the expansion port and at the target manhole (see Fig. 1). Segmented wire ionization chambers measured the beam divergence and allowed to discard, offline, beam pulses with unsatisfactory steering. The proportion of pions and kaons in the secondary beam was measured by a differential Cherenkov counter, situated at the expansion port, which was placed into the beam at regular time intervals. The monitoring of the secondary beam, the calibration of the ionization chambers and the analysis of the Cherenkov counter data were performed by the CCFRR collaboration.* Details may be found in Ref. 4. To obtain the neutrino flux at the bubble chamber on a burst-by-burst basis, that is, the correct normalization to the bubble chamber exposures, the relevant flux monitor information was combined with a beam transport and decay Monte Carlo. In Fig. 2, the energy-weighted neutrino flux at the bubble chamber, as a function of the radial distance from the beam center, is compared to a similar distribution obtained by the CCFRR collaboration. Detailed comparisons of this kind indicate that possible differences in the cross section arising from the flux normalization are smaller than 1%.

---

* We are grateful to the CCFRR collaboration for supplying us with all the relevant information concerning the neutrino flux and for many critical discussions.

2.2 The 15-ft Bubble Chamber

The Fermilab 15-ft bubble chamber was filled with a 59% atomic neon-hydrogen mix. This mixture is an almost perfect "isoscalar" target with a slight proton excess of 3.4%. The bubble chamber operated in a 30 kG magnetic field. The liquid density was monitored during data taking by the bubble chamber support group: Liquid samples were submitted to a chromatographic analysis. The average density determined by this method was $\langle\rho\rangle = 0.71 \pm 0.04$ g cm^{-3}. An independent determination of $\langle\rho\rangle$ was obtained from the data: Using the range of protons stopping in the liquid and their momentum from the curvature in the magnetic field, the value $\langle\rho\rangle = 0.715 \pm 0.020$ g cm^{-3} was obtained, in good agreement with the chromatographic analysis. The error includes systematic uncertainties of 2%. This density corresponds to a radiation length of $\approx$ 40 cm and an interaction length of $\approx$ 125 cm; thus, for a typical charged current neutrino interaction, the muon leaves the bubble chamber, while hadrons are likely to interact.

3. DATA ANALYSIS

3.1 Selection of Charged Current Events

At the five settings of the secondary beam momentum quoted in Section 2.1, a total of 98,000 bubble chamber frames was recorded. All frames were scanned for possible neutrino interactions but for the cross section determination, only 78,000 frames with a valid flux monitor information were retained. A fiducial volume requirement assured a high detection efficiency for charged current interactions.

The scanning efficiency was obtained from double scanning 60% of the frames. It was found to be (93 ± 4)%.

Neutrino interactions were selected by requiring the total visible energy of the event to be more than 10 GeV and the angle of the total visible momentum vector with the neutrino direction to be less than 45°. These requirements greatly reduced backgrounds from cosmic radiation and from neutral particles produced before the bubble chamber. At this stage, the number of events was 1043. To select charged current interactions, the fastest leaving negative track was taken to be a muon; its momentum was required to be higher than 2 GeV/c. The charged current sample obtained in this way contained 830 events.

3.2 Neutral Current Background

The principal background to the above charged current sample came from neutral current interactions in which a π^- with a momentum above 2 GeV/c leaves the bubble chamber without interacting in the liquid. The method of determining this "hadronic punchthrough" background is described below.

Because all positive tracks in the data sample are hadrons, the ratio L^+/I^+ of the number of leaving to interacting positive tracks is a measure of the hadronic punchthrough;

it is a property of the bubble chamber liquid and depends on the track momentum.* This ratio, multiplied by the number of interacting negative tracks, I_p^-, of a given momentum and summed over all momenta,** gives L_h^-, the number of leaving negative hadrons:

$$L_h^- = \sum_p (L^+/I^+)_p \cdot I_p^- \quad .$$

For a given event, only the fastest of the leaving negative hadrons is simulating a muon; thus to obtain the number of fake charged current events, one has to subtract from L_h^- the number of successive leaving negative tracks with $P > 2$ GeV/c. In this way, a neutral current background of $(12 \pm 4)\%$ was obtained. The method has the additional merit to include also the background from neutral particles other than neutrinos.

An alternative method consists of disregarding, for each event in the charged current sample, the fastest leaving negative track which is supposed to be a muon. The truncated events simulate the hadronic part of neutral current events; thus, asking for a second leaving negative track with a momentum above 2 GeV/c determines the hadronic punchthrough probability. Using this probability in an iterative way, a punchthrough background of $(9 \pm 2)\%$ was obtained. The two methods having given compatible results, we used the combined result of $(10 \pm 2)\%$.

3.3 Other Backgrounds

For the cross section determination, one has to disregard events for which the neutrino originated upstream of the momentum selecting slit (see Fig. 1) of the narrow band beam, because the corresponding parent pions or kaons are usually not detected by the ionization chambers, thus not considered in the neutrino flux measurement. This "wide band background" was directly measured by the CCFRR collaboration by closing the momentum selecting slit.† Their result of $(2.5 \pm 0.5)\%$ was used in the present analysis.[4]

Interactions produced by cosmic radiation were largely suppressed by the total energy and angle requirements. The residual background was found to be $(0.4 \pm 0.4)\%$ by counting events with the momentum vector pointing into the backward direction with respect to the neutrinos.

---

* The fact that positive hadrons contain some protons while negative hadrons are mostly pions was taken into account by studying interactions of pions from identified K^o decays.

** One has to include all events, with and without a muon, in the track counting.

† The corresponding bubble chamber data were statistically insignificant.

3.4 Losses Due to Kinematic Cuts

Corrections due to the kinematic cuts were small. The visible energy cut at 10 GeV implied a loss of $(1 \pm 1)\%$. To correct for the cut at 2 GeV/c on the muon momentum, each event was weighted according to the unsampled part of the scaling-y distribution.* The total correction, averaged over all events, amounted to $(3.6 \pm 1)\%$.

The possibility of losing events with low track multiplicity at the scanning stage was investigated. Events with a μ^- and one positive track are expected from the quasi-elastic reaction, $\nu + n \rightarrow \mu^- + p$, and from some single pion channels; their contribution to the total cross section was estimated to be $(3 \pm 1)\%$. By counting these "low topology" events in the sample, this loss was estimated to be $(1 \pm 1)\%$.

Table 1 summarizes all corrections to the charged current data sample. The number on the bottom line is the corrected number of charged current events which enter into the cross section determination.

3.5 Determination of the Cross Section Slope

Assuming a linear rise with neutrino energy (E_ν), the cross section slope is given by:

$$\sigma_\nu/E_\nu = N_{cc}/W \ .$$

N_{cc} is the corrected number of charged current events in Table 1, and

$$W = [\text{Nucleons/Fiducial Volume}] * \sum_{i=1}^{N_\nu} E_\nu^{\,i} \cdot \ell_i$$

is the corresponding normalization obtained from the beam transport and decay Monte Carlo. The summation runs over all generated neutrinos; $E_\nu^{\,i}$ is the energy of the i^{th} neutrino and ℓ_i the potential pathlength of the i^{th} neutrino within the fiducial volume. The three sources of neutrinos,

$$\pi^+ \rightarrow \mu^+\nu_\mu \ , \quad K^+ \rightarrow \mu^+\nu_\mu \ , \text{ and } K^+ \rightarrow \pi^o\mu^+\nu_\mu \ ,$$

have been considered. Normalizing to the total number of parent pions and kaons detected by the ionization chambers during the active time of the experiment, one obtains:

$$W = (1298 \pm 66)\ 10^{38}\text{GeV/cm}^2 \ .$$

The error is due to uncertainties in the flux monitoring and beam composition measurement (4%), to uncertainties of the Monte Carlo parameters (1%), and to the error on the bubble chamber liquid density (3%). Using the above value of W, one obtains $\sigma_\nu/E_\nu = 0.635 * 10^{-38}\text{cm}^2/\text{GeV}$. To express the cross section slope for any "isoscalar" target, one has to correct for the slight proton excess of the

---

* For the y distribution $(d\sigma/dy) \sim [(1+B)+(1-B)(1-y)^2]$ was used with $B = 0.8$.

neon-hydrogen mixture. Using $2\sigma_p = \sigma_n$, the final result

$$\sigma_\nu/E_\nu = (0.64 \pm 0.02 \pm 0.04)10^{-38}\ \text{cm}^2/\text{GeV}$$

was obtained. The first error is statistical, coming essentially from the number of observed charged current events and the second includes all systematic uncertainties related to the corrections of Table 1, the flux monitoring and the liquid density. The total systematic error reduces to 0.02 if the uncertainties of the flux monitoring, common to this experiment and the CCFRR measurement, are not considered.

3.6 Consistency Checks and Searches for Systematic Biases

The five settings of the secondary beam momentum constitute five independent experiments. The corresponding results, presented in Table 2, are consistent with each other.

In order to test the long term stability over several months of data taking, we calculated σ_ν/E_ν for each of the 55 rolls of film. The distribution of results did not show any trend with time and the spread of results was consistent with the statistical expectation.

To detect possible biases related to specific parts of the fiducial volume, we studied the distribution of event vertices along the beam direction, along the horizontal and vertical coordinates transverse to the beam and in radial bins around the beam center. No significant deviation from expectations was found.

The scanning was performed by the three institutions of the collaboration. In order to check the homogeneity of the scanning, we determined σ_ν/E_ν separately for the three institutions and found consistent results.

4. CROSS SECTION AS A FUNCTION OF NEUTRINO ENERGY

In the previous sections, the cross section slope, averaged over all neutrino energies, was determined.

To determine the energy dependence of σ_ν/E_ν, one has to reconstruct the energy of the incoming neutrino for each event. One approach is to correct the "visible" energy for the undetected energy carried by neutral particles. The resulting energy resolution is typically $\Delta E_\nu/E_\nu \approx 0.15$ for $E_\nu < 100$ GeV and higher for $E_\nu > 100$ GeV, with asymmetric tails.

A more reliable approach is based on the dichromatic property of the narrow band beam which permits one to determine the neutrino energy from the radial position of the interaction vertex. The neutrino energy is related to the radial distance, R, from the center of the neutrino beam by the expression:

$$E_\nu \approx \frac{2\gamma\, E_\nu^*}{1+\gamma^2 (R/L)^2}\ ,$$

where E_ν^* is the neutrino energy in the parent's center of mass system, L is the mean separation between the parent's decay point and the neutrino interaction point, and γ is the Lorentz boost factor of the parent particle. This method implies a decision for each event regarding the parent (pion or kaon) of the neutrino. Because for the predominant decay modes, $\pi \to \mu\nu$ and $K \to \mu\nu$, the c.m.s. neutrino energies are very different, [$E_\nu^*(\pi) = 0.03$ GeV, whereas $E_\nu^*(K) = 0.236$ GeV], a crude determination of the event energy is sufficient to reach this decision. A convenient method of separating the events from the two sources of neutrinos is based on the quantity:

$$S = (E_{vis} - E_\pi^R)/(E_K^R - E_\pi^R) \quad ,$$

where E_{vis} is the visible energy increased by 5% to correct for the undetected neutral particles; E_π^R and E_K^R are the energies predicted from the radial position, assuming the parent of the neutrino to be a pion or kaon, respectively. The distribution of events as a function of S (Fig. 3) shows a clear clustering around the expected values of 0 and 1.

The cross section slope as a function of neutrino energy is shown in Fig. 4. The error bars include the uncertainty related to the use of S to separate the two sources of neutrinos. The data do not indicate any deviation from a linear rise of the cross section.

5. DISCUSSION

We reported on a new determination of the charged current cross section slope, σ_ν/E_ν , from a bubble chamber experiment which was running concurrently with the CCFRR counter experiment. Based on 830 events, the cross section was found to rise linearly with neutrino energy within the interval 10 GeV $\leq E_\nu \leq$ 240 GeV; the slope was found to be:

$$\sigma_\nu/E_\nu = (0.64 \pm 0.05)\ 10^{-38}\ cm^2 GeV^{-1} \quad .$$

Without being in disagreement with the CCFRR result, this measurement favors the lower value obtained by earlier experiments. This can be seen from Table 3 where our result is presented together with previously available neutrino and anti-neutrino results. The table includes the anti-neutrino result of the Berkeley-Fermilab-Hawaii bubble chamber measurement, which also favors the lower value obtained by earlier experiments.

References

1 Review of Particle Properties, Rev. Mod. Phys. 52, #2 (1980). For cross sections and related refs., see p. 554.

2 R. Blair et al, Proc. of the 1981 Int. Conf. on Neutrino Physics and Astrophysics, Maui, Hawaii, Vol. I, p. 311.
R. Blair et al, to be published in Phys. Rev. Letters.

3 Contribution to this conference by H. Bingham.

4 R. Blair, Ph.D. Thesis (1982), Caltech, Pasadena, CA. "A Total Cross Section and ν-Distribution Measurement for Muon-Type Neutrinos and Antineutrinos in Iron".

Table 1: Corrections to the Charged Current Event Sample

	Correction	Events
Uncorrected sample:		830 ± 29
Scanning efficiency:	93 ± 4%	
Low-multiplicity losses:	1 ± 1%	
Neutral current background:	10 ± 2%	
Wide band background:	2.5 ± 0.5%	
Cosmic radiation:	0.4 ± 0.4%	
Visible energy cut:	1 ± 1%	
Muon momentum cut:	3.6 ± 1%	
Corrected number of charged current events:		823 ± 50

Table 2: σ_ν/E_ν for Specific Settings of the Secondary Beam Momentum

Momentum (GeV)	σ_ν/E_ν (10^{-38} cm^2.GeV^{-1})
120	0.58 ± 0.06
140	0.65 ± 0.04
165	0.62 ± 0.04
200	0.68 ± 0.06
250	0.64 ± 0.05

Table 3: Summary of High Energy Neutrino and Anti-Neutrino Charged Current Cross Sections

Experiment	$\sigma_{\bar{\nu}}/E_{\bar{\nu}}$ $[10^{-38}cm^2GeV^{-1}]$	σ_{ν}/E_{ν} $[10^{-38}cm^2GeV^{-1}]$
CDHS[a]	0.30 ± 0.02	0.62 ± 0.03
CHARM[b]	$0.301\pm0.008\pm0.016$	$0.604\pm0.009\pm0.031$
BEBC[c]	$0.303\pm0.010\pm0.011$	$0.663\pm0.012\pm0.025$
CCFRR[d]	$0.350\pm0.004\pm0.022$	$0.701\pm0.004\pm0.025$
BFH[e]	0.30 ± 0.02	
This Experiment		$0.64\pm0.02\pm0.04$

[a] J.G.H. deGroot et al, Z. Phys. C1, 143 (1978).
[b] M. Jonker et al, Phys. Lett. 99B, 265 (1981).
[c] P. Fritze, Proc. of the 1981 Int. Conf. on Neutrino Physics and Astrophysics, Maui, Hawaii, Vol. I, p. 344.
[d] Ref. 3.
[e] Ref. 4.

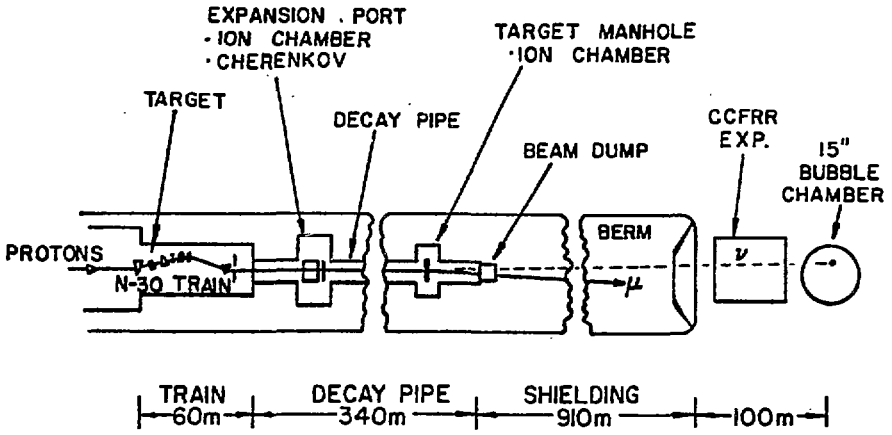

Fig. 1 Layout of the Fermilab narrow band neutrino/anti-neutrino beam. The approximate positions of the 15-ft bubble chamber and of the CCFRR counter experiment are indicated.

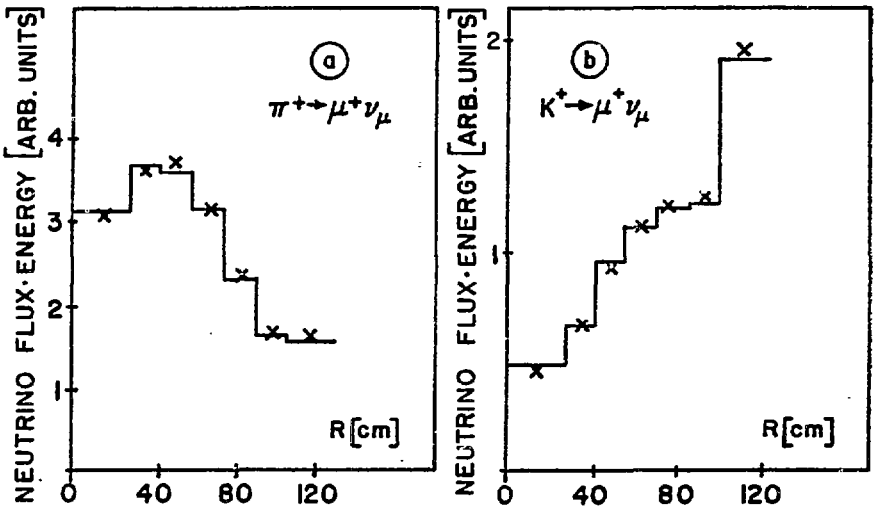

Fig. 2 Energy-weighted neutrino flux at the bubble chamber in radial bins around the beam center. Secondary momentum: 200 GeV/c. Neutrinos from a) $\pi^+ \to \mu^+ \nu_\mu$; b) $K^+ \to \mu^+ \nu_\mu$. Full historgram: this experiment; crosses: CCFRR experiment.

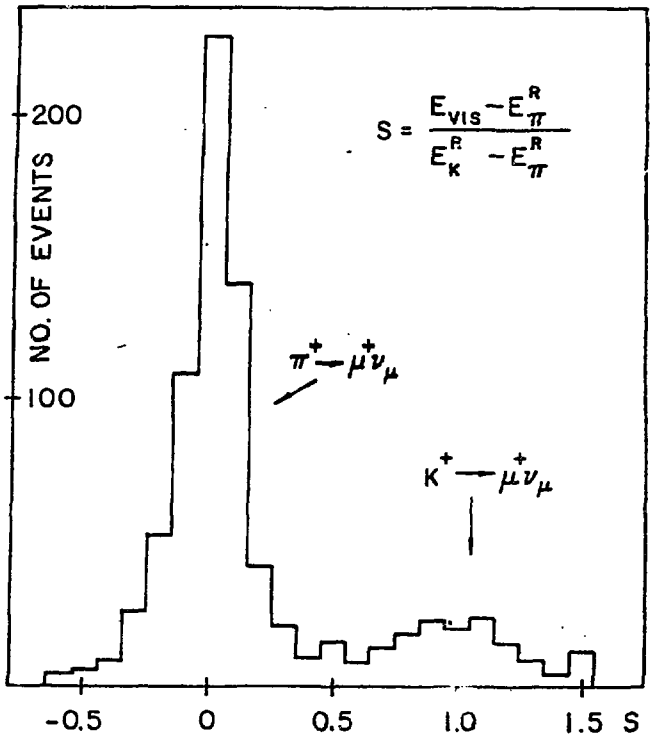

Fig. 3 Distribution of charged current events as a function of S. Events from $\pi^+ \rightarrow \mu^+ \nu_\mu$ and $K^+ \rightarrow \mu^+ \nu_\mu$ are clustered at the values S = 0 and 1, respectively.

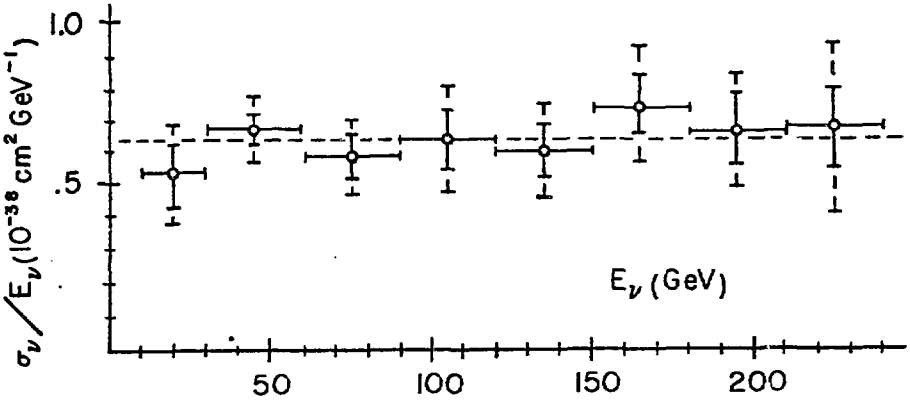

Fig. 4 Cross section slope as a function of neutrino energy. Inner error bars: statistical only; outer error bars: include systematic effects. The mean value of σ_ν/E_ν=0.64 is indicated.